catalysts

MDPI

Article

Hydrogenolysis of Glycerol to 1,2-Propanediol and Ethylene Glycol over Ru-Co/ZrO_2 Catalysts

Jian Feng [1,*], Youquan Zhang [2], Wei Xiong [1], Hao Ding [1] and Bai He [1]

[1] College of Chemistry and Chemical Engineering, Chongqing University of Science & Technology, Chongqing 401331, China; xiongwcq@163.com (W.X.); dinghao_dh@yeah.net (H.D.); hbai2004@126.com (B.H.)

[2] Guangxi Key Laboratory of Petrochemical Resource Processing and Process Intensification Technology, School of Chemistry and Chemical Engineering, Guangxi University, Nanning 530004, China; zyq1968@163.com

* Correspondence: fengjianscu@163.com; Tel.: +86-23-6502-3739

Academic Editor: Keith Hohn

Received: 2 February 2016; Accepted: 22 March 2016; Published: 25 March 2016

Abstract: A series of ZrO_2 supported Ru-Co bimetallic catalysts were prepared and evaluated for the hydrogenolysis of glycerol. The Ru-Co/ZrO_2 bimetallic catalyst combines the advantages of both Ru and Co, exhibiting high activity and good selectivity to 1,2-propanediol. The X-ray diffraction (XRD) and TEM results show that higher calcination temperature leads to lower reducibility of cobalt oxides and larger metal particle size, which is responsible for the decrease of glycerol conversion. Increasing the reduction temperature causes an inhibition effect on the catalytic activity, but it is beneficial to promote the 1,2-propanediol selectivity. The low temperature (<300 °C) reduction can prevent the growth of metal particles, resulting in higher activity. Co oxide is an important component for the good performance of Ru-Co/ZrO_2. The reaction temperature, hydrogen pressure, and glycerol concentration have significant effects on the catalytic performance of the Ru-Co/ZrO_2 catalyst.

Keywords: glycerol; hydrogenolysis; ruthenium; cobalt; 1,2-propanediol; ethylene glycol

1. Introduction

In the past few decades, because of the growing shortage of fossil fuels, the utilization of renewable fuels has become a fundamental way to implement sustainable development. Biodiesel is such a widely-used renewable fuel that can be produced from biomass-derived plant oils or animal fats. The rapid development of biodiesel production forms large quantities of glycerol as a byproduct. Therefore, the conversion of glycerol to other high value-added products has received increased attention [1]. One attractive route for the transformation of glycerol involves the catalytic hydrogenolysis to 1,2-propanediol (1,2-PDO). This diol is an important chemical for the production of polyesters, resins, and polyurethanes. Although cost-competitiveness is yet a key barrier, the hydrogenolysis of glycerol to 1,2-PDO is indisputably a promising green technology.

Hydrogenolysis of glycerol can be achieved over various heterogeneous metal catalysts. These catalysts and their catalytic performances have been summarized and discussed in several recent reviews [2–5]. Among the reported catalysts, Ru is usually found to be very active even under relatively low temperature [3,5]. Nevertheless, Ru is also active for the excessive hydrogenolysis reaction, resulting in some undesired degradation products, such as ethylene glycol (EG), 1-propanol, 2-propanol, ethanol, methanol, and even methane.

With the purpose of improving the performance of Ru, especially the selectivity to 1,2-PDO, efforts are devoted to Ru-based bimetallic catalysts. The synergistic effect between Ru and the other metal usually make the catalytic performance of the bimetallic catalysts better than that of the

monometallic catalysts. Ru-Cu [6–9] and Ru-Re [10–12] were two of the mainly reported bimetallic catalysts. Cu is well known to suppress C–C bond cleavage while still showing high rates of C–O bond cleavage in hydrogenolysis reactions. However, the Cu component usually leads to lower activity and particle agglomeration during the reaction [7,9,13]. In some cases, Ru and Cu in the bimetallic catalyst even work independently without obvious synergistic effect [6]. Using Ru-Cu/NaY and Ru-Cu/HY as catalyst, the dominating product is 1-propanol rather than 1,2-PDO [8]. The research group of He [10,11] studied the hydrogenolysis of glycerol over a series of bimetallic Ru-Re catalysts, including Ru-Re/SiO_2, Ru-Re/ZrO_2, Ru-Re/TiO_2, Ru-Re/H-β, Ru-Re/H-ZSM5. The addition of the Re component can improve the dispersion of Ru and generate ReO_x species with acidic sites. Ru-Re bimetallic catalysts exhibited higher hydrogenolysis activity as compared to the monometallic Ru catalyst, while the monometallic Re catalyst showed almost no catalytic activity for the reaction [11,12]. Unfortunately, the selectivity to 1,2-PDO over Ru-Re bimetallic catalysts was not satisfactory (<50%), which would restrict its practical application.

Recently, Co [14–16] has been reported effective for the glycerol hydrogenolysis reaction. Co species can interact with MgO, layered double hydroxides, or ZnO, thereby enhancing the stability of the catalysts. More importantly, Co exhibits very low activity for the cleavage of the C–C bond, resulting in high selectivity to 1,2-PDO [16]. However, the catalytic activity of Co is much lower than that of Ru in most cases. Mauriello and co-workers have demonstrated that the interaction between Pd and Co can modify the electronic properties of Pd, which enhances the catalytic performance for both the conversion of glycerol and the selectivity to 1,2-PDO [17,18]. This effect may also work for the Ru-Co bimetallic catalyst.

On the basis of our previous works on monometallic Ru catalysts [19–22], we envisage combining the advantages of Ru and Co to obtain a more efficient Ru-Co bimetallic catalyst. Our preliminary study [23] screened out ZrO_2 as a good support for the selective hydrogenolysis of glycerol. Therefore, in this work, a series of ZrO_2 supported Ru-Co bimetallic catalysts were prepared and evaluated for the hydrogenolysis of glycerol. The calcination and reduction treatments remarkably influenced the catalyst structure and the catalytic performance. Ru-Co/ZrO_2 was found to be an efficient catalyst for the hydrogenolysis of glycerol to 1,2-PDO under optimized conditions.

2. Results and Discussion

2.1. Catalytic Performance of Monometallic and Bimetallic Catalysts

Firstly, the glycerol hydrogenolysis reaction was performed using the Ru/ZrO_2 and Co/ZrO_2 monometallic catalysts, as well as the Ru-Co/ZrO_2 bimetallic catalyst. The results are comparatively presented in Table 1. A blank reaction was also conducted with neat ZrO_2; however, almost no conversion was observed in the absence of a metal catalyst, indicating that ZrO_2 is unable to catalyze the hydrogenolysis of glycerol independently and that the metal catalyst is necessary for the reaction. As shown in Table 1, Ru/ZrO_2 exhibited high activity and low selectivity to 1,2-PDO, resulting in large amounts of degradation products (EG and monohydroxy-alcohols). The results are consistent with other monometallic Ru-based catalysts [9,20]. In contrast, Co/ZrO_2 showed low activity, but the selectivity to 1,2-PDO was high, up to 83.2%. The addition of Co metal to the Ru-based catalyst remarkably enhanced the selectivity to 1,2-PDO, although the activity was slightly decreased in comparison with that of the monometallic Ru catalyst.

Some physical properties of the as-prepared catalysts are listed in Table 2. Inductively coupled plasma-atomic emission spectrometry (ICP-AES) results show that the metal weight loadings are near to the set value described in the experimental section. The Brunauer-Emmett-Teller (BET) surface areas of all the catalysts were decreased after the preparation procedures. The bimetallic catalyst possesses bigger metal particles as compared to the monometallic catalysts. Because the catalytic performance of different metals is associated with their intrinsic property [4,5], no obvious relations can be found between the determined physical properties and the catalytic performance. In spite of this, our preliminary study [23] on the effect of Ru/Co molar ratio has demonstrated that the catalytic activity decreased with increasing Co loading, while a contrary trend was found for the selectivity

to 1,2-PDO. The best performance can be obtained by the catalyst with a Ru/Co molar ratio of 1:2; thus, this catalyst was used in the present work. It was also reported that Cu has a similar effect on the catalytic performance of Ru-Cu/ZrO_2 [8].

Table 1. Catalytic performance of the prepared catalysts in glycerol hydrogenolysis [a].

Catalyst [b]	Conversion (%)	Selectivity (%) [c]		LCB (%)
		1,2-PDO	EG	
ZrO_2	<1.0	-	-	-
Ru/ZrO_2	67.5	41.1	29.8	18.2
Ru-Co/ZrO_2 [23]	56.2	70.3	18.0	10.7
Co/ZrO_2	22.7	83.2	7.3	4.1

[a] Reaction conditions: 3 mL glycerol aqueous solution (20 wt. %), 180 °C, 5 MPa, 10 h, 50 mg catalyst. 1,2-PDO: 1,2-propanediol, EG: ethylene glycol, LCB: loss of carbon balance; [b] The catalysts were calcined at 350 °C and reduced at 250 °C; [c] Other products: 1-propanol, 2-propanol, ethanol, methanol and 1,3-propanediol.

Table 2. Some characterization results from inductively coupled plasma-atomic emission spectrometry (ICP-AES), N_2 adsorption, and TEM.

Catalyst [a]	Metal Loading (wt. %)	BET Surface Area (m^2/g)	TEM Particle Size (nm)
ZrO_2	-	65	-
Ru/ZrO_2	5.06	57	8.1
Ru-Co/ZrO_2 [b]	Ru: 4.97, Co: 5.75	48	9.8
Co/ZrO_2	5.12	52	6.3

[a] The catalysts were calcined at 350 °C and reduced at 250 °C; [b] Molar ratio of Ru:Co = 1:2 (this is the best ratio according to our previous study [23]).

Combination of the results in Table 1 and our study on the effect of Ru/Co molar ratio reveals that the product selectivity is remarkably influenced by the Co component in the Ru-Co/ZrO_2 bimetallic catalyst. Co can promote the cleavage of C–O bond, which is responsible for the increase of 1,2-PDO selectivity in the glycerol hydrogenolysis reaction. In addition, the Co content in the Ru-Co/ZrO_2 bimetallic catalyst differs slightly with that in the Co/ZrO_2 monometallic catalyst (5.75 wt. % and 5.12 wt. % respectively, Table 2), but the activity of Ru-Co/ZrO_2 was much higher than that of Co/ZrO_2. This indicates that the Ru-Co bimetallic catalyst functions more like monometallic Ru in terms of catalytic activity. The Ru-Co/ZrO_2 bimetallic catalyst combines the high activity of Ru and the good selectivity of Co.

2.2. Effect of Calcination Temperature

The calcination temperature is of importance for the decomposition of metal salt precursors and the formation of various phases [24]. Table 3 presents the catalytic performance of Ru-Co/ZrO_2 calcined at different temperatures. These catalysts were all reduced at 250 °C. As the calcination temperature elevated from 250 °C to 550 °C, there was a uniform decrease in the conversion of glycerol, from 58.7% to 29.1%. The selectivity to 1,2-PDO and EG changed slightly when the calcination temperatures were above 350 °C.

Table 3. Effect of calcination temperature on the catalytic performance of Ru-Co/ZrO_2 [a].

Calcination Temperature (°C)	Conversion (%)	Selectivity (%)		LCB (%)
		1, 2-PDO	EG	
250	58.7	64.8	24.4	15.0
350	56.2	70.3	18.0	10.7
450	43.5	68.9	15.3	7.9
550	29.1	71.8	16.9	5.2

[a] Reaction conditions: 3 mL glycerol aqueous solution (20 wt. %), 180 °C, 5 MPa, 10 h, 50 mg catalyst (reduced at 250 °C).

Figure 1 shows the XRD patterns of the Ru-Co/ZrO_2 catalysts calcined at different temperatures. The support, ZrO_2, is in the crystalline phase of baddeleyite (JCPDS Card #86-1450). The peak intensity increases with increasing calcination temperature, suggesting that higher calcination temperature leads to higher crystallinity and larger particle size. The diffraction peaks at 2θ = 38.5° and 44.2° (partially overlapped with a peak of ZrO_2 at 2θ = 44.8°) are attributed to metallic Ru (JCPDS Card #89-3942). The diffraction peaks at 2θ = 34.0° (mostly overlapped with a peak of ZrO_2 at 2θ = 34.2°) and 39.5° can be assigned to CoO (JCPDS Card #75-0419). As can be seen from Figure 1, the phases of metallic Ru and CoO were present in all the catalyst samples. It is interesting to note that Co_3O_4 (the strongest diffraction peak at 2θ = 36.9°, JCPDS Card #74-1656) existed in the sample calcined at 550 °C, which indicates higher calcination temperature is unfavorable to the reduction of cobalt oxides. Previous works [14,25] also demonstrate that increasing the calcination temperature can result in decreased reducibility of the cobalt oxides. This may be one of the reasons for the decreased glycerol conversion at higher calcination temperature (Table 3).

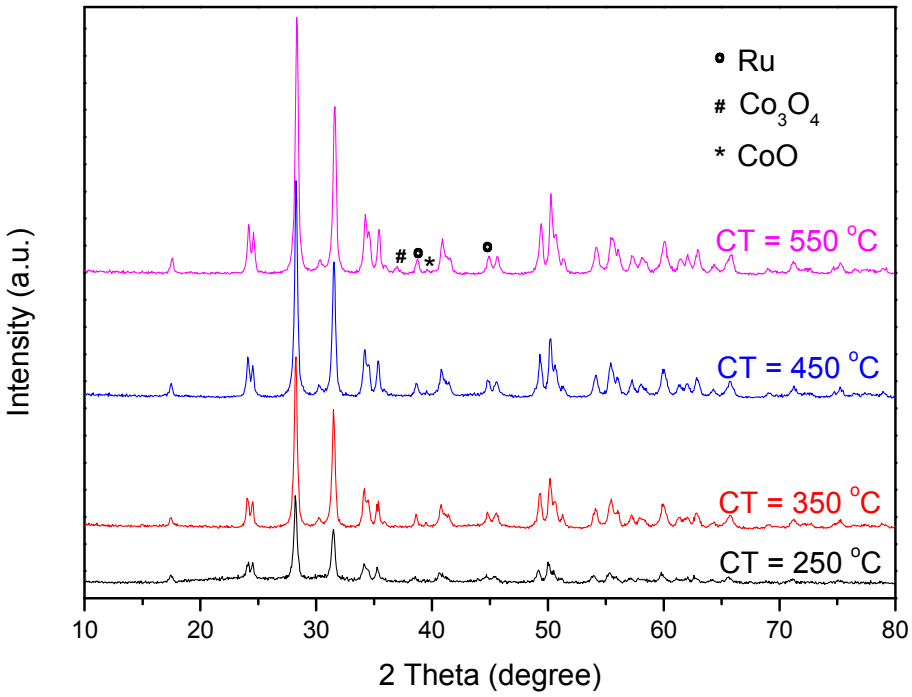

Figure 1. X-ray Diffraction (XRD) patterns of Ru-Co/ZrO_2 calcined at different temperatures. The catalysts were reduced at 250 °C after calcination. CT: calcination temperature.

Figure 2 illustrates the TEM images of the Ru-Co/ZrO_2 catalysts calcined at different temperatures. As can be clearly seen from the images, the nanosized particles (including metal and metal oxide) are well dispersed on the ZrO_2 support when the calcination temperature is 250 °C (Figure 2a) or 350 °C (Figure 2b), whereas the dispersion is not good when the calcination temperature increases to 450 °C (Figure 2c) or 550 °C (Figure 2d). This indicates that higher temperature treatment will lead to the aggregation of metal and metal oxide particles. In fact, the average particle size in Figure 2a,b was determined to be about 8.3 nm and 9.8 nm, respectively. However, it is hard to estimate the particle size in Figure 2c,d because the TEM image clarity is not very good. These results are consistent with the XRD experiments (Figure 1) as discussed above. The growth in the metal particle size may be another reason for the decreased glycerol conversion at higher calcination temperature (Table 3).

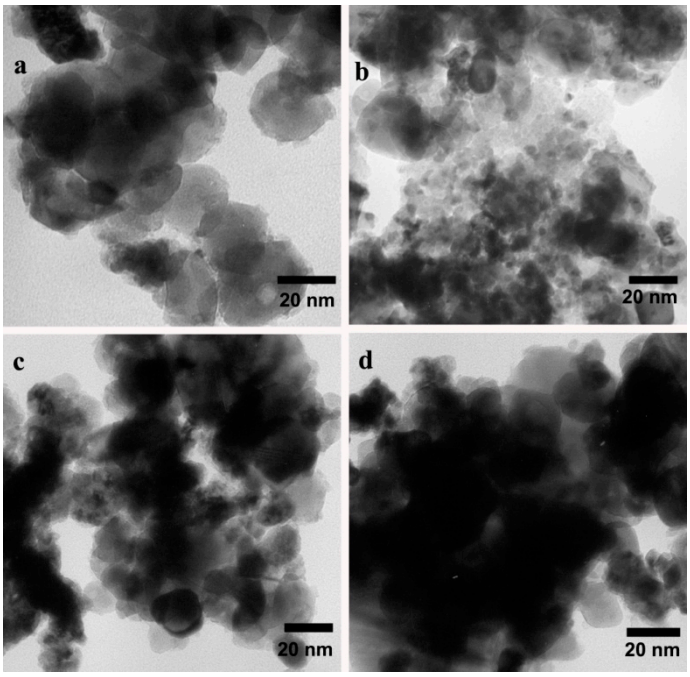

Figure 2. TEM images of Ru-Co/ZrO_2 calcined at: (**a**) 250 °C; (**b**) 350 °C; (**c**) 450 °C and (**d**) 550 °C. The catalysts were reduced at 250 °C after calcination.

2.3. Effect of Reduction Temperature

Reduction is a crucial step in the catalyst preparation process. The reduction temperature can influence the catalyst reducibility, thereby influencing the catalytic performance [18,26]. The reaction results of glycerol hydrogenolysis using the Ru-Co/ZrO_2 catalysts reduced at different temperatures are presented in Table 4. These catalysts were all calcined at 350 °C. Obviously, increasing the reduction temperature causes an inhibition effect on the catalytic activity, but it is beneficial to promote the 1,2-PDO selectivity and to restrain the production of EG. To be specific, as the reduction temperature was raised from 250 °C to 500 °C, the conversion of glycerol decreased from 56.2% to 14.8%, while the 1,2-PDO selectivity increased from 70.3% to 78.5%. It is worth noting that the unreduced catalyst exhibited even higher activity than that of the catalysts reduced at 400 °C and 500 °C. One reasonable explanation for this is that the catalyst can be reduced *in situ* in the glycerol hydrogenolysis reaction under hydrogen atmosphere. However, the unreduced catalyst obtained the lowest selectivity to 1,2-PDO, which may be related to the chloride ions contained in the catalyst (the unreduced catalyst was not washed with deionized water, see the Experimental section). The chloride ion was testified to go against the formation of 1,2-PDO by Vasiliadou and co-workers [27].

Table 4. Effect of reduction temperature on the catalytic performance of Ru-Co/ZrO_2 [a].

Reduction Temperature (°C)	Conversion (%)	Selectivity (%)		LCB (%)
		1, 2-PDO	EG	
Unreduced	43.0	62.2	26.7	5.9
250	56.2	70.3	18.0	10.7
300	42.6	71.8	16.5	8.4
400	28.7	74.0	10.3	5.5
500	14.8	78.5	11.6	3.8

[a] Reaction conditions: 3 mL glycerol aqueous solution (20 wt. %), 180 °C, 5 MPa, 10 h, 50 mg catalyst (calcined at 350 °C).

Figure 3 depicts the XRD patterns of the Ru-Co/ZrO_2 catalysts reduced at different temperatures. As has been discussed above, the diffraction peaks at 2θ = 38.5° and 39.5° are attributed to metallic Ru and CoO, respectively (other characteristic peaks are overlapped with the peaks of ZrO_2). Due to the weak intensity of corresponding diffraction peaks, we are unable to calculate the particle size by the Scherrer equation. Even so, it can be seen from Figure 3 that the peak intensity gradually enhanced with increasing reduction temperature, implying that the crystal particles became larger at higher reduction temperatures. This changing trend is similar to the catalysts calcined at different temperatures (Figure 1). Our previous work [20] on the hydrogenolysis of glycerol using Ru/TiO_2 catalyst has elucidated that raising the reduction temperature will cause the growth of Ru particle size, thereby decreasing the catalyst activity. As a matter of fact, high temperature treatments usually lead to the growth of metal or metal oxide particles [28]. Combination of the catalytic performances in Table 4 shows that the growth of metal particle size is a logical explanation for the lower activity at higher reduction temperature. Moreover, the low temperature (<300 °C) reduction can prevent the growth of metal particles, resulting in relatively higher activity.

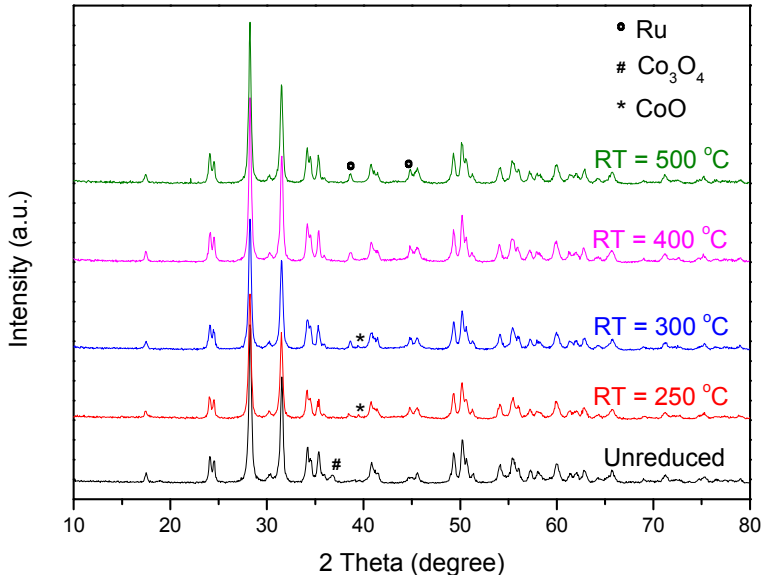

Figure 3. XRD patterns of Ru-Co/ZrO_2 reduced at different temperatures. The catalysts were calcined at 350 °C before reduction. RT: reduction temperature.

In addition, the phase of metallic Ru (2θ = 38.5°) appeared in all the reduced catalysts, which indicates that ruthenium oxides are more easily reduced. The Co_3O_4 phase (2θ = 36.9°) only existed in the unreduced sample, but CoO (2θ = 39.5°) presented in the samples reduced at 250 °C and 300 °C. This implies the reduction of Co_3O_4 is a two-step process, which corresponds to the reduction of Co_3O_4 to CoO, and then the reduction of CoO to metallic Co. No obvious diffraction peaks of metallic Co (the strongest diffraction peak at 2θ = 47.4°, JCPDS Card #89-7373) can be observed in the XRD patterns, probably because the Co particles are too small to be detected.

Figure 4 presents the temperature programmed reduction (TPR) profiles of the Ru/ZrO_2, Co/ZrO_2, and Ru-Co/ZrO_2 catalysts. The Ru/ZrO_2 sample showed a single reduction peak at around 217 °C, which can be assigned to the reduction of RuO_2 to Ru metal [10,29]. The Co/ZrO_2 catalyst exhibited two distinct reduction maxima with one at 334 °C and another at 460 °C. The former reduction peak is attributed to the reduction of Co_3O_4 to CoO, and the second one corresponds to the reduction of CoO to metallic Co. This reduction characteristic is in good agreement with other studies using SiO_2 [30,31] and ZrO_2 [32] as support. As for the Ru-Co/ZrO_2 bimetallic catalyst, the TPR pattern presented a maximum at 245 °C and two shoulder peaks at 196 °C and 312 °C. Obviously, the reducibility of ruthenium and cobalt species was enhanced, suggesting that there is a synergistic

effect between Ru and Co in the Ru-Co/ZrO_2 bimetallic catalyst [30,31]. This phenomenon can be explained by a mechanism commonly known as "intraparticle hydrogen spillover" [31,33]. According to the TPR result of Ru-Co/ZrO_2, the reduction of Co_3O_4 to CoO started from about 210 °C, and this process was accompanied by the reduction of CoO to metallic Co. The cobalt oxides can be reduced to metallic Co at around 330 °C. This reduction characteristic can reasonably explain the XRD result in Figure 3: CoO appeared in the samples reduced at 250 °C and 300 °C because of the reduction of Co_3O_4, and then CoO disappeared in the samples reduced at 400 °C and 500 °C due to the reduction of CoO to metallic Co.

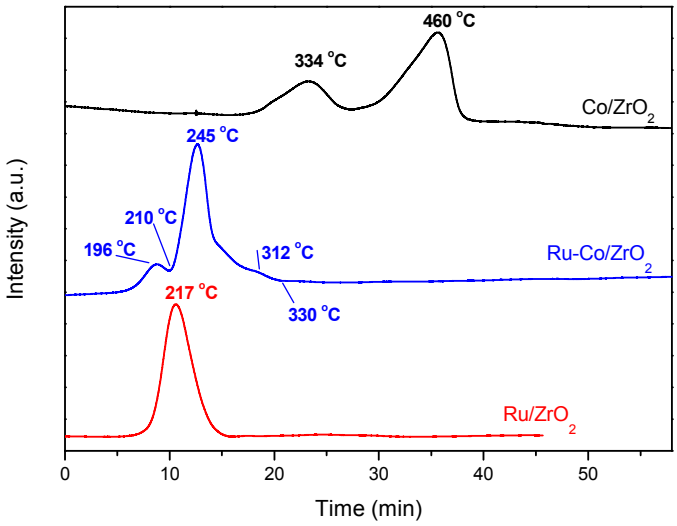

Figure 4. Temperature programmed reduction (TPR) profiles of the monometallic and bimetallic catalysts. The catalysts were calcined at 350 °C before TPR experiments.

A typical Co 2p X-ray photoelectron spectroscopy (XPS) spectrum of Ru-Co/ZrO_2 reduced at 250 °C is shown in Figure 5. For reference, the Co 2p XPS spectra of Ru-Co/ZrO_2 reduced at 300 °C, 400 °C, and 500 °C are also provided in Figure S1, Figure S2, and Figure S3 (Supplementary Material), respectively. As can be seen in Figure 5, there are two doublets in the XPS pattern. One doublet (dotted line) with binding energy at 786.9 eV and 802.4 eV is attributed to the satellite peaks. Another doublet (solid line) can be assigned to CoO (binding energy: Co $2p_{3/2}$ = 780.8 eV, Co $2p_{1/2}$ = 796.2 eV) [34,35]. The presence of satellite peaks is a typical feature for Co^{2+}, and they cannot be observed for Co^{3+} [16]. Almost the same XPS results were obtained for Ru-Co/ZrO_2 reduced at 300 °C (Figure S1), suggesting that CoO is the main cobalt phase in the catalysts reduced at 250 °C and 300 °C. This agrees well with the XRD and TPR results. Nevertheless, the binding energy only shifts a little lower (Co $2p_{3/2}$ = 780.5 eV) for the catalysts reduced at 400 °C (Figure S2) and 500 °C (Figure S3), indicating that the cobalt element is also in oxidation state. This may be owing to the re-oxidization of metal surface that occurred during the catalyst storage before the XPS experiments [16]. The Ru 3d XPS spectra of Ru/ZrO_2 and Ru-Co/ZrO_2 (reduced at 250 °C) are shown in Figure S4 and Figure S5 in the Supplementary Material, respectively. The Ru $3d_{5/2}$ peak of Ru/ZrO_2 and Ru-Co/ZrO_2 is almost at the same binding energy position (about 280.3 eV), indicating that there is no obvious change in the electronic properties of Ru after the addition of Co. This may be the reason that the bimetallic Ru-Co catalyst works more like a monometallic Ru catalyst in terms of catalytic activity (Table 1).

Based on the catalytic reaction results in Table 4, the optimal tradeoff between the glycerol conversion and the 1,2-PDO selectivity can be obtained by the catalyst calcined at 350 °C and reduced at 250 °C. From the XRD, TPR, and XPS results, it can be seen that the Co component is present mostly as the phase of CoO. This Co oxide may be beneficial for the formation and transformation of intermediate, resulting in good performance of the corresponding Ru-Co/ZrO_2 catalyst. However, the exact role of Co oxide needs further investigation.

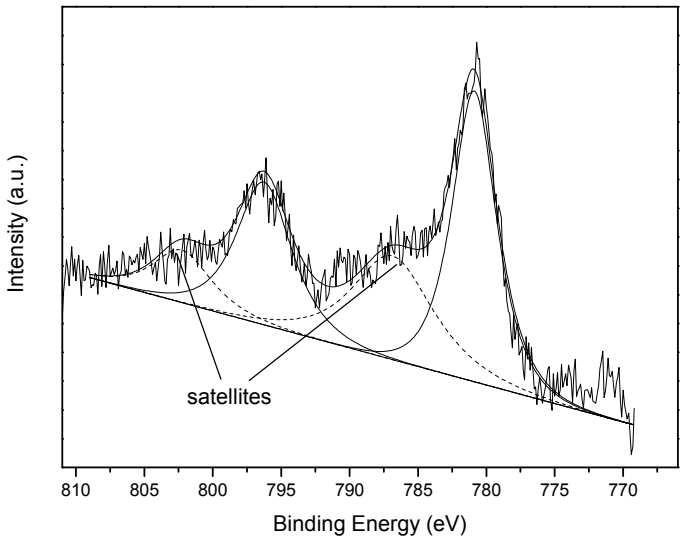

Figure 5. Co 2p X-ray photoelectron spectroscopy (XPS) spectrum of Ru-Co/ZrO_2 reduced at 250 °C.

2.4. Effect of Reaction Conditions

According to the above results and discussions, Ru-Co/ZrO_2 calcined at 350 °C and reduced at 250 °C exhibited the best catalytic performance in the glycerol hydrogenolysis reaction, giving satisfying activity and good 1,2-PDO selectivity. Therefore, this catalyst was selected for further study.

The effect of reaction temperature on the glycerol conversion and product selectivity was studied in the range of 140–200 °C. The results are depicted in Figure 6. As expected, the conversion of glycerol increased remarkably with increasing reaction temperature. The selectivity to 1,2-PDO gradually increased when the reaction temperature was raised from 140 °C to 180 °C, after that it began to decrease. Correspondingly, the selectivity to EG changed slightly before 180 °C, but then it became higher. This indicates that overhigh reaction temperature favors the cleavage of the C–C bond, leading to the formation of degradation products. Therefore, high selectivity to 1,2-PDO requires an optimal reaction temperature, as was found at 180 °C in Figure 6.

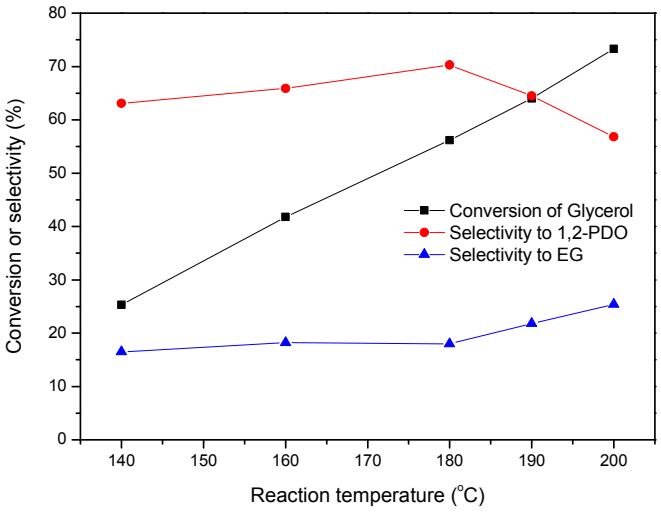

Figure 6. Effect of reaction temperature on glycerol hydrogenolysis over Ru-Co/ZrO_2. Reaction conditions: 3 mL glycerol aqueous solution (20 wt. %), 5 MPa, 10 h, 50 mg catalyst (calcined at 350 °C, reduced at 250 °C).

Figure 7 shows the effect of hydrogen pressure on the catalytic performance of Ru-Co/ZrO_2. The hydrogen pressure dramatically influenced the glycerol conversion, while it only slightly affected

the product selectivity. The conversion of glycerol increased monotonously with increasing hydrogen pressure. The solubility of hydrogen in water is proportional to the hydrogen pressure [36]. Therefore, the increasing glycerol conversion may be caused by the enhanced concentration of hydrogen in the aqueous solution with increasing pressure. Similar results have been obtained over other catalysts such as Co/MgO [14].

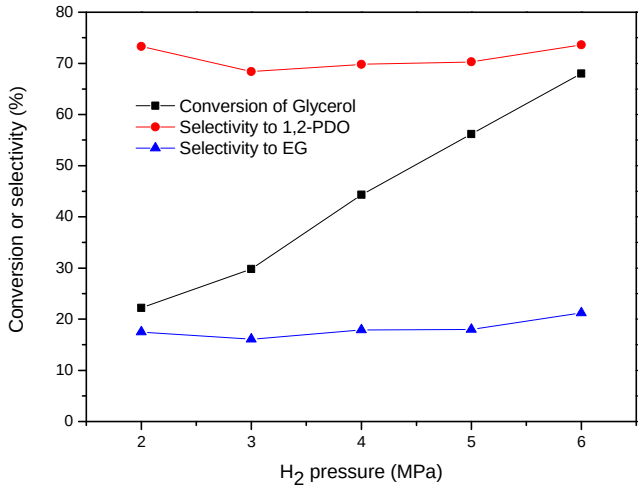

Figure 7. Effect of hydrogen pressure on glycerol hydrogenolysis over Ru-Co/ZrO_2. Reaction conditions: 3 mL glycerol aqueous solution (20 wt. %), 180 °C, 10 h, 50 mg catalyst (calcined at 350 °C, reduced at 250 °C).

As we know, glycerol is a liquid with high viscosity. Overhigh concentration of glycerol will cause substrate diffusion problems because of the mass transfer limitation [21]. The effect of glycerol concentration on the catalytic performance of Ru-Co/ZrO_2 is presented in Figure 8. As the glycerol concentration increased, the conversion of glycerol decreased. This changing tendency is easy to understand: the substrate amount increases with increasing glycerol concentration, while the available number of catalytic sites (*i.e.*, the amount of catalyst) is constant. Interestingly, the selectivities to 1,2-PDO and EG were almost unchanged with the change in glycerol concentration, which is in accord with previous findings over monometallic Ru [37,38] and Co [14] catalysts.

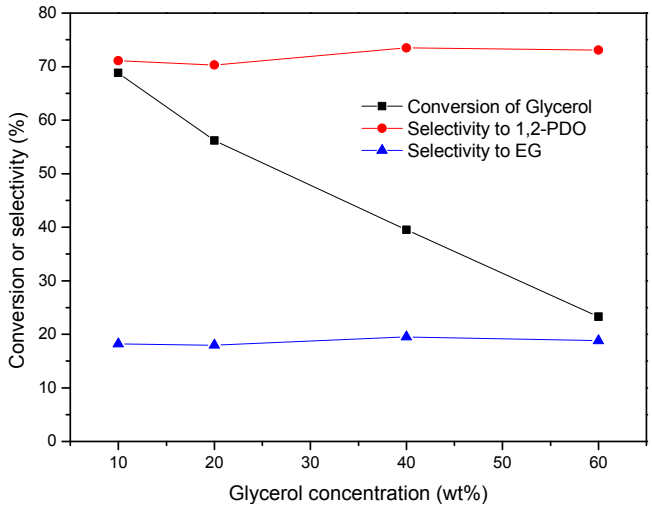

Figure 8. Effect of glycerol concentration on glycerol hydrogenolysis over Ru-Co/ZrO_2. Reaction conditions: 3 mL glycerol aqueous solution, 180 °C, 5 MPa, 10 h, 50 mg catalyst (calcined at 350 °C, reduced at 250 °C).

3. Experimental Section

3.1. Catalyst Preparation

The support, ZrO_2, was purchased as analytical reagent (AR) sample from KeLong chemical (Chengdu, China). The Ru-Co bimetallic catalysts were prepared by co-impregnation method. The loading of Ru was kept at 5 wt. %, based on the amount of $RuCl_3 \cdot 3H_2O$ (Kunming Institute of Precious Metals, Kunming, China). Typical procedures for the preparation of Ru-Co/ZrO_2 (5 wt. % Ru, 5.8 wt. % Co) catalyst with a molar ratio of Ru:Co = 1:2 are described as follows. Weighed amounts of ZrO_2 were impregnated with the aqueous solution of $RuCl_3 \cdot 3H_2O$ and $Co(NO_3)_2 \cdot 6H_2O$ (KeLong chemical, Chengdu, China). After impregnation, the solvent was removed under reduced pressure on a rotary evaporator. The resulting powder was dried in vacuum at 110 °C for 10 h. The dried samples were calcined in a muffle furnace at different temperatures (250 °C, 350 °C, 450 °C, and 550 °C) for 4 h. Subsequently, the calcined samples were reduced with flowing hydrogen in a fixed-bed quartz reactor at different temperatures (250 °C, 300 °C, 400 °C, and 500 °C) for 4 h. The reduced samples were washed repeatedly with deionized water to remove chloride ions, and then dried at 60 °C in vacuum for 10 h to obtain the final catalysts. For comparison, the monometallic Ru/ZrO_2 (5 wt. %) and Co/ZrO_2 (5 wt. %) catalysts were prepared in the same way.

3.2. Catalyst Characterization

The weight loading of Ru or Co was determined by inductively coupled plasma-atomic emission spectrometry (ICP-AES) (IRIS Intrepid, Thermal Elemental, Boston, MA, USA). BET surface areas of the catalysts were measured on an auto adsorption/desorption analyzer (ZXF-6, Northwest Chemical Industry, Xi'an, China) using nitrogen as adsorbate.

The X-ray diffraction (XRD) measurements were performed on an X'Pert Pro MPD X-ray diffractometer (Philips, Amsterdam, Netherlands) equipped with a Cu Kα radiation source (λ = 0.15406 nm). About 50 mg of catalyst samples were pressed in the sample holder. The operating voltage and current were 40 kV and 25 mA, respectively. The XRD patterns were obtained with a scan rate of 2 s/step and a step size of 0.05° (2θ). The particle size of corresponding crystalline phase was determined by XRD using Scherrer equation ($d = 0.9\lambda/\beta\cos\theta$) if the peaks were intense enough. Transmission electron microscopy (TEM) was used to determine the particle size and the morphology of the catalyst samples. The TEM images were obtained by JEM-1200EX at 100 kV (JEOL, Tokyo, Japan). The sample was ultrasonically suspended in ethanol and deposited on a Cu grid recovered with a thin layer of carbon. The X-ray photoelectron spectroscopy (XPS) experiments were carried out on an X-ray photoelectron spectrometer (XSAM800, Kratos, Manchester, UK), employing Mg Kα radiation. The X-ray source was operated at 12 kV and 12 mA.

The reduction characteristics of the catalysts were studied by temperature programmed reduction (TPR). The TPR experiments were carried out on a homemade apparatus equipped with a U-shaped quartz reactor and a thermal conductivity detector (Haixin, Shanghai, China). To remove the adsorbed water and other contaminants, 100 mg of the calcined catalyst sample in the reactor was pretreated in flowing He at 350 °C for 1 h, followed by cooling to 100 °C. After the pretreatment, the gas was switched to 10% H_2/He at a flow rate of 30 mL/min, and the temperature was raised to 750 °C (10 °C/min).

3.3. Catalytic Experiments

Hydrogenolysis of glycerol was carried out in a 60 mL stainless steel autoclave equipped with a magnetic stirrer and an electric temperature controller. The catalyst and glycerol aqueous solution were charged into the autoclave. The reactor was sealed and purged repeatedly with hydrogen to eliminate air. Then, the reactor was pressurized to the necessary hydrogen pressure and heated to the desired reaction temperature. Details of the reaction conditions are described for each experiment in the text. A full list of products and selectivities are shown in Tables S1–S3 in the Supplementary Material.

After the reaction, the reactor was cooled to room temperature. The liquid-phase products were analyzed by HPLC (SHIMADZU, Tokyo, Japan) using an Aminex HPX-87H (Bio-Rad, Hercules, CA, USA) column and a refractive index detector. The mobile phase was sulphuric acid with a concentration of 5 mM. The gas products were analyzed by GC (GC-9790, Wenling, China) equipped with a 601 molecular sieve packed column and a thermal conductivity detector. The liquid products detected were 1,2-propanediol (1,2-PDO), ethylene glycol (EG), 1-propanol, 2-propanol, ethanol, methanol, and trace amounts of 1,3-propanediol. Gas products contained small amounts of CH_4 and CO_2. The selectivity denotes the selectivity in liquid products [10,11]. The loss of carbon balance is calculated as the percentage of missing carbon (the carbon except the liquid phase) accounted for at the end of the reaction. Because the reactor was not equipped to analyze the gas and liquid products simultaneously, a certain amount of gas phase products were inevitably lost during liquid sampling [39]. To be specific, the glycerol conversion and product selectivity were calculated on carbon basis according to the following equations:

$$\text{Conversion of glycerol}\,(\%) = \frac{\text{moles of glycerol consumed}}{\text{moles of glycerol initially charged}} \times 100$$

$$\text{Selectivity}\,(\%) = \frac{\text{moles of carbon in specific product}}{\text{moles of carbon in all detected products}} \times 100$$

4. Conclusions

The addition of Co component to the Ru-based catalyst remarkably enhanced the selectivity to 1,2-PDO for the glycerol hydrogenolysis reaction. The bimetallic Ru-Co catalyst functions more like monometallic Ru in terms of catalytic activity. Ru-Co/ZrO_2 calcined at 350 °C and reduced at 250 °C exhibited the best catalytic performance. The XRD and TEM results show that the growth in the metal particle size may be the reason for the lower activity at higher calcination or reduction temperature. The TPR results indicate that a synergistic effect between Ru and Co exists in the Ru-Co/ZrO_2 bimetallic catalyst. Co oxide is an important component for the good performance of Ru-Co/ZrO_2 catalyst. The reaction temperature, hydrogen pressure, and glycerol concentration have significant effects on the catalytic performance of the catalyst. The reaction conditions used in this work are mild, but the 1,2-PDO selectivity is not very satisfying as compared to some Ru-Cu catalysts [8,9]. More investigations are under progress to further improve the catalytic activity and selectivity.

Supplementary Materials: The following are available online at www.mdpi.com/2073-4344/6/4/51/s1, Figure S1: Co 2p XPS spectrum of Ru-Co/ZrO_2 reduced at 300 °C; Figure S2: Co 2p XPS spectrum of Ru-Co/ZrO_2 reduced at 400 °C; Figure S3: Co 2p XPS spectrum of Ru-Co/ZrO_2 reduced at 500 °C; Figure S4: Ru 3d XPS spectrum of Ru/ZrO_2 reduced at 250 °C; Figure S5: Ru 3d XPS spectrum of Ru-Co/ZrO_2 reduced at 250 °C; Table S1: Catalytic performance of the prepared catalysts in glycerol hydrogenolysis; Table S2: Effect of calcination temperature on the catalytic performance of Ru-Co/ZrO_2; Table S3: Effect of reduction temperature on the catalytic performance of Ru-Co/ZrO_2.

Acknowledgments: This work was supported by the National Natural Science Foundation of China (No. 21302237), the Basic and Frontier Research Program of Chongqing (cstc2014jcyjA90004), and the Opening Project of Guangxi Key Laboratory of Petrochemical Resource Processing and Process Intensification Technology (2013K006).

Author Contributions: Jian Feng and Youquan Zhang conceived and designed the experiments; Jian Feng and Hao Ding performed the experiments; Wei Xiong and Bai He analyzed the data; Jian Feng wrote the paper. All authors reviewed the manuscript.

Conflicts of Interest: The authors declare no conflict of interest.

References

1. Zhou, C.H.; Beltramini, J.N.; Fan, Y.X.; Lu, G.Q. Chemoselective catalytic conversion of glycerol as a biorenewable source to valuable commodity chemicals. *Chem. Soc. Rev.* **2008**, *37*, 527–549. [CrossRef] [PubMed]

2. Wang, Y.L.; Zhou, J.X.; Guo, X.W. Catalytic hydrogenolysis of glycerol to propanediols: A review. *RSC Adv.* **2015**, *5*, 74611–74628. [CrossRef]
3. Nakagawa, Y.; Tomishige, K. Heterogeneous catalysis of the glycerol hydrogenolysis. *Catal. Sci. Technol.* **2011**, *1*, 179–190. [CrossRef]
4. Martin, A.; Armbruster, U.; Gandarias, I.; Arias, P.L. Glycerol hydrogenolysis into propanediols using *in situ* generated hydrogen—A critical review. *Eur. J. Lipid Sci. Technol.* **2013**, *115*, 9–27. [CrossRef]
5. Feng, J.; Xu, B. Reaction mechanisms for the heterogeneous hydrogenolysis of biomass-derived glycerol to propanediols. *Prog. React. Kinet. Mech.* **2014**, *39*, 1–15. [CrossRef]
6. Jiang, T.; Zhou, Y.X.; Liang, S.G.; Liu, H.Z.; Han, B.X. Hydrogenolysis of glycerol catalyzed by Ru-Cu bimetallic catalysts supported on clay with the aid of ionic liquids. *Green Chem.* **2009**, *11*, 1000–1006. [CrossRef]
7. Vasiliadou, E.S.; Lemonidou, A.A. Investigating the performance and deactivation behaviour of silica-supported copper catalysts in glycerol hydrogenolysis. *Appl. Catal. A* **2011**, *396*, 177–185. [CrossRef]
8. Liu, H.Z.; Liang, S.G.; Jiang, T.; Han, B.X.; Zhou, Y.X. Hydrogenolysis of glycerol to 1,2-propanediol over Ru-Cu bimetals supported on different supports. *Clean Soil Air Water* **2012**, *40*, 318–324. [CrossRef]
9. Salazar, J.B.; Falcone, D.D.; Pham, H.N.; Datye, A.K.; Passos, F.B.; Davis, R.J. Selective production of 1,2-propanediol by hydrogenolysis of glycerol over bimetallic Ru-Cu nanoparticles supported on TiO_2. *Appl. Catal. A* **2014**, *482*, 137–144. [CrossRef]
10. Ma, L.; He, D.H. Influence of catalyst pretreatment on catalytic properties and performances of Ru-Re/SiO_2 in glycerol hydrogenolysis to propanediols. *Catal. Today* **2010**, *149*, 148–156. [CrossRef]
11. Ma, L.; Li, Y.M.; He, D.H. Glycerol hydrogenolysis to propanediols over Ru-Re/SiO_2: Acidity of catalyst and role of Re. *Chin. J. Catal.* **2011**, *32*, 872–876. [CrossRef]
12. Torres, A.; Roy, D.; Subramaniam, B.; Chaudhari, R.V. Kinetic modeling of aqueous-phase glycerol hydrogenolysis in a batch slurry reactor. *Ind. Eng. Chem. Res.* **2010**, *49*, 10826–10835. [CrossRef]
13. Wang, S.; Yin, K.H.; Zhang, Y.C.; Liu, H.C. Glycerol hydrogenolysis to propylene glycol and ethylene glycol on zirconia supported noble metal catalysts. *ACS Catal.* **2013**, *3*, 2112–2121. [CrossRef]
14. Guo, X.H.; Li, Y.; Shi, R.J.; Liu, Q.Y.; Zhan, E.S.; Shen, W.J. Co/MgO catalysts for hydrogenolysis of glycerol to 1,2-propanediol. *Appl. Catal. A* **2009**, *371*, 108–113. [CrossRef]
15. Guo, X.H.; Li, Y.; Song, W.; Shen, W.J. Glycerol hydrogenolysis over Co catalysts derived from a layered double hydroxide precursor. *Catal. Lett.* **2011**, *141*, 1458–1463. [CrossRef]
16. Rekha, V.; Sumana, C.; Douglas, S.P.; Lingaiaha, N. Understanding the role of Co in Co-ZnO mixed oxide catalysts for theselective hydrogenolysis of glycerol. *Appl. Catal. A* **2015**, *491*, 155–162. [CrossRef]
17. Musolino, M.G.; Scarpino, L.A.; Mauriello, F.; Pietropaolo, R. Glycerol hydrogenolysis promoted by supported palladium catalysts. *ChemSusChem* **2011**, *4*, 1143–1150. [CrossRef] [PubMed]
18. Mauriello, F.; Ariga, H.; Musolino, M.G.; Pietropaolo, R.; Takakusagi, S.; Asakura, K. Exploring the catalytic properties of supported palladium catalysts in the transfer hydrogenolysis of glycerol. *Appl. Catal. B* **2015**, *166–167*, 121–131. [CrossRef]
19. Feng, J.; Wang, J.B.; Zhou, Y.F.; Fu, H.Y.; Chen, H.; Li, X.J. Effect of base additives on the selective hydrogenolysis of glycerol over Ru/TiO_2 catalyst. *Chem. Lett.* **2007**, *36*, 1274–1275. [CrossRef]
20. Feng, J.; Fu, H.Y.; Wang, J.B.; Li, R.X.; Chen, H.; Li, X.J. Hydrogenolysis of glycerol to glycols over ruthenium catalysts: Effect of support and catalyst reduction temperature. *Catal. Commun.* **2008**, *9*, 1458–1464. [CrossRef]
21. Feng, J.; Xiong, W.; Jia, Y.; Wang, J.B.; Liu, D.R.; Chen, H.; Li, X.J. Hydrogenolysis of glycerol to 1,2-propanediol over Ru/TiO_2 catalyst. *Chin. J. Catal.* **2011**, *32*, 1545–1549. [CrossRef]
22. Feng, J.; Xiong, W.; Xu, B.; Jiang, W.D.; Wang, J.B.; Chen, H. Basic oxide-supported Ru catalysts for liquid phase glycerol hydrogenolysis in an additive-free system. *Catal. Commun.* **2014**, *46*, 98–102. [CrossRef]
23. Feng, J.; Xu, B.; Jiang, W.D.; Xiong, W.; Wang, J.B. Hydrogenolysis of glycerol on supported Ru-Co bimetallic catalysts. *Adv. Mater. Res.* **2012**, *549*, 297–300. [CrossRef]
24. Abasaeed, A.E.; Al-Fatesh, A.S.; Naeem, M.A.; Ibrahim, A.A.; Fakeeha, A.H. Catalytic performance of CeO_2 and ZrO_2 supported Co catalysts for hydrogen production via dry reforming of methane. *Int. J. Hydrogen Energy* **2015**, *40*, 6818–6826. [CrossRef]
25. Song, S.H.; Lee, S.B.; Bae, J.W.; Prasad, P.S.S.; Jun, K.W.; Shul, Y.G. Effect of calcination temperature on the activity and cobalt crystallite size of Fischer-Tropsch Co-Ru-Zr/SiO_2 catalyst. *Catal. Lett.* **2009**, *129*, 233–239. [CrossRef]

26. Priya, S.S.; Kumar, V.P.; Kantam, M.L.; Bhargava, S.K.; Periasamy, S.; Chary, K.V.R. Metal–acid bifunctional catalysts for selective hydrogenolysis of glycerol under atmospheric pressure: A highly selective route to produce propanols. *Appl. Catal. A* **2015**, *498*, 88–98. [CrossRef]
27. Vasiliadou, E.S.; Heracleous, E.; Vasalos, I.A.; Lemonidou, A.A. Ru-based catalysts for glycerol hydrogenolysis—Effect of support and metal precursor. *Appl. Catal. B* **2009**, *92*, 90–99. [CrossRef]
28. Yin, H.F.; Ma, Z.; Zhu, H.G.; Chi, M.F.; Dai, S. Evidence for and mitigation of the encapsulation of gold nanoparticles within silica supports upon high-temperature treatment of Au/SiO_2 catalysts: Implication to catalyst deactivation. *Appl. Catal. A* **2010**, *386*, 147–156. [CrossRef]
29. Park, S.J.; Bae, J.W.; Oh, J.H.; Chary, K.V.R.; Prasad, P.S.S.; Jun, K.W.; Rhee, Y.W. Influence of bimodal pore size distribution of $Ru/Co/ZrO_2$-Al_2O_3 during Fischer-Tropsch synthesis in fixed-bed and slurry reactor. *J. Mol. Catal. A* **2009**, *298*, 81–87. [CrossRef]
30. Song, S.H.; Lee, S.B.; Bae, J.W.; Prasad, P.S.S.; Jun, K.W. Influence of Ru segregation on the activity of Ru-Co/γ-Al_2O_3 during FT synthesis: A comparison with that of Ru-Co/SiO_2 catalysts. *Catal. Commun.* **2008**, *9*, 2282–2286. [CrossRef]
31. Huang, L.; Xu, Y. Studies on the interaction between ruthenium and cobalt in supported catalysts in favor of hydroformylation. *Catal. Lett.* **2000**, *69*, 145–151. [CrossRef]
32. Zhang, X.H.; Su, H.Q.; Yang, X.Z. Catalytic performance of a three-dimensionally ordered macroporous Co/ZrO_2 catalyst in Fischer-Tropsch synthesis. *J. Mol. Catal. A* **2012**, *360*, 16–25. [CrossRef]
33. Tsubaki, N.; Sun, S.; Fujimoto, K. Different functions of the noble metals added to cobalt catalysts for Fischer-Tropsch synthesis. *J. Catal.* **2001**, *199*, 236–246. [CrossRef]
34. John, F.M.; William, F.S.; Peter, E.S.; Kenneth, D.B. *Handbook of X-ray Photoelectron Spectroscopy*, 1st ed.; Physical Electronics, Inc.: Eden Prairie, MN, USA, 1995; pp. 82–83.
35. Oku, M.; Hirokawa, K. X-Ray photoelectron spectroscopy of Co_3O_4, Fe_3O_4, Mn_3O_4 and related compounds. *J. Electron Pectrosc. Relat. Phenom.* **1976**, *8*, 475–481. [CrossRef]
36. Dasari, M.A. Catalytic Conversion of Glycerol and Sugar Alcohols to Value-Added Products. Ph.D. Thesis, University of Missouri-Columbia, Columbia, MO, USA, 2006.
37. Alhanash, A.; Kozhevnikova, E.F.; Kozhevnikov, I.V. Hydrogenolysis of glycerol to propanediol over Ru: Polyoxometalate bifunctional catalyst. *Catal. Lett.* **2008**, *120*, 307–311. [CrossRef]
38. Balaraju, M.; Rekha, V.; Prasad, P.S.S.; Devi, B.L.A.P.; Prasad, R.B.N.; Lingaiah, N. Influence of solid acids as co-catalysts on glycerol hydrogenolysis to propylene glycol over Ru/C catalysts. *Appl. Catal. A* **2009**, *354*, 82–87. [CrossRef]
39. Maris, E.P.; Davis, R.J. Hydrogenolysis of glycerol over carbon-supported Ru and Pt catalysts. *J. Catal.* **2007**, *249*, 328–337. [CrossRef]

© 2016 by the authors; licensee MDPI, Basel, Switzerland. This article is an open access article distributed under the terms and conditions of the Creative Commons by Attribution (CC-BY) license (http://creativecommons.org/licenses/by/4.0/).